AD-A107 739 ROCHESTER INST OF TECH NY DEPT OF ELECTRICAL ENGINEERING F/G 17/9
ENHANCEMENT OF POLES IN SPECTRAL ANALYSIS.(U)
NOV 81 F I TSENG, T K SARKAR N00014-79-C-0598
UNCLASSIFIED TR-81-5 NL

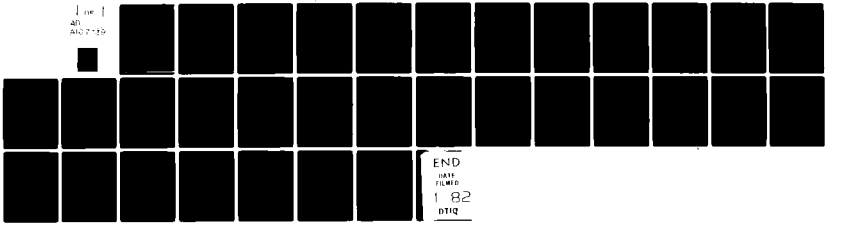

END
DATE FILMED
1 82
DTIC

LEVEL II

(10)

ENHANCEMENT OF POLES IN SPECTRAL ANALYSIS

by

Fung I. Tseng

Tapan K. Sarkar

Manuscript received

This work has been supported by Office of Naval Research under contract N00014-79-C-0598.

The authors are with
Department of Electrical Engineering
Rochester Institute of Technology
Rochester, New York 14623

UNCLASSIFIED

SECURITY CLASSIFICATION OF THIS PAGE (When Data Entered)

REPORT DOCUMENTATION PAGE		READ INSTRUCTIONS BEFORE COMPLETING FORM
1. REPORT NUMBER: TR-81-5	2. GOVT ACCESSION NO. AD-A108	3. RECIPIENT'S CATALOG NUMBER
4. TITLE (and Subtitle): Enhancement of Poles in Spectral Analysis		5. TYPE OF REPORT & PERIOD COVERED: Technical Report No. 5
		6. PERFORMING ORG. REPORT NUMBER
7. AUTHOR(s): F.I.Tseng and T.K.Sarkar		8. CONTRACT OR GRANT NUMBER(s): N00014-79-C-0598
9. PERFORMING ORGANIZATION NAME AND ADDRESS: Dept. of Electrical Engineering, Rochester Institute of Technology, Rochester, New York 14623		10. PROGRAM ELEMENT, PROJECT, TASK AREA & WORK UNIT NUMBERS: 61153N RR021-01, RR021-01-01, NR371-014
11. CONTROLLING OFFICE NAME AND ADDRESS: Department of the Navy, Office of Naval Research, Arlington, Virginia 22217		12. REPORT DATE: November 1981
		13. NUMBER OF PAGES: 30
14. MONITORING AGENCY NAME & ADDRESS(if different from Controlling Office)		15. SECURITY CLASS. (of this report): UNCLASSIFIED
		15a. DECLASSIFICATION/DOWNGRADING SCHEDULE

16. DISTRIBUTION STATEMENT (of this Report)

DISTRIBUTION STATEMENT A
Approved for public release;
Distribution Unlimited

17. DISTRIBUTION STATEMENT (of the abstract entered in Block 20, if different from Report)

18. SUPPLEMENTARY NOTES

19. KEY WORDS (Continue on reverse side if necessary and identify by block number)
1) Poles
2) FFT
3)Chirp z-Transform
4) Spectral Analysis
5) Superresolution

20. ABSTRACT (Continue on reverse side if necessary and identify by block number)

This paper presents a new technique for detecting a small pole in the presence of a nearby strong pole. By simultaneously applying the chirp z-transform (CZT) and a recently developed window, the new technique is shown to be able to detect and resolve a small pole. The CZT is efficient since it employs the Fast Fourier Transform (FFT) to evaluate a convolution. But unlike the FFT which is limited to the evaluation of the spectrum on the jw axis, the CZT can evaluate the z-transform on the whole complex plane.

DD FORM 1 JAN 73 1473 EDITION OF 1 NOV 65 IS OBSOLETE
S/N 0102-LF-014-6601

UNCLASSIFIED
SECURITY CLASSIFICATION OF THIS PAGE (When Data Entered)

20.

And with the use of the new window, which is designed to have a near-sidelobe level of any specified value, the CZT is shown to be able to resolve two closely spaced poles with a large difference in amplitudes. Unlike the Prony's Method, the new technique does not require predetermining the system order. No matrix inversion or solution of polynomial roots is required. Further, the new technique is a linear operation, thus even under noisy environments it yields accurate, stable results for extraction of poles from transient response data.

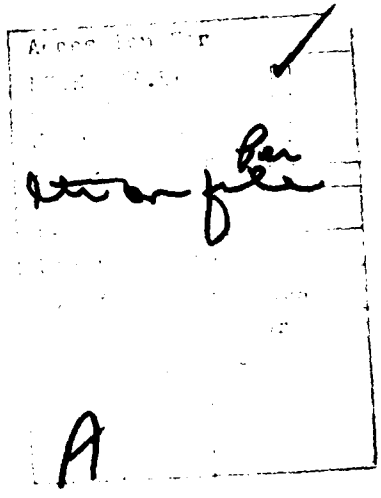

ABSTRACT

This paper presents a new technique for detecting a small pole in the presence of a nearby strong pole. By simultaneously applying the chirp z-transform (CZT) and a recently developed window, the new technique is shown to be able to detect and resolve a small pole.

The CZT is efficient since it employs the Fast Fourier Transform (FFT) to evaluate a convolution. But unlike the FFT which is limited to the evaluation of the spectrum on the jw asix, the CZT can evaluate the z-transform on the whole complex plane. And with the use of the new window, which is designed to have a near-sidelobe level of any specified value, the CZT is shown to be able to resolve two closely spaced poles with a large difference in amplitudes.

Unlike the Prony's method, the new technique does not require predetermining the system order. No matrix inversion or solution of polynomial roots is required. Further, the new technique is a linear operation, thus even under noisy environments it yields accurate, stable results for extraction of poles from transient response data.

I. Introduction

In target identification one often illuminates the target by a wideband pulse. One then characterizes the target by the complex natural resonances extracted from the electromatnetic response. This paper presents a new technique for detecting a small pole in the presence of a nearby strong pole.

In recent years the singularity expansion method has been applied to express the electromagnetic response in an expansion of complex resonances of the target [1] It has been shown that the dominant complex natural resonances of a target are a minimal set of parameters

that define the overall physical properties of the target [2]. To extract the complex resonances the Prony's method has been applied successfully for noiseless data [3]. Recently, the pencil-of-function method has been shown to be effective in dealing with noisy data for extraction of the poles [4]. These techniques essentially involve nonlinear data processing, requiring the solution of polynomial roots and matrix inversion. The key problem is the determination of the system order [5], which is complicated due to the presence of noise in data.

To circumvent the complexity of these methods, an alternative technique for extracting the complex poles is investigated. By taking advantage of the simplicity and efficiency of the FFT algorithm, one can modify the FFT so that it can be employed to evaluate the z-transform of the time sequence along a general contour on the complex plane. The modified FFT or the chirp z-transform (CZT) therefore plays the role in a discrete system, played by the Lapalce Transform in continuous systems. [6]. Because the time sequence is finite, the CZT has the leakage effect. To suppress the leakage effect, a recently developed window [7], which is designed to have a low near-sidelobe level, is simultaneously applied with the CZT. Two examples are given to illustrate the technique, which is shown to be able to detect and resolve a small pole in the presence of a nearby strong pole. The new technique does not require pre-determining the order of the system. No matrix inversion or solution of polynomial roots is required. Furthermore, since the CZT is a linear operation, it yields stable results even under noisy environments.

II The Chirp z-Transform

Consider a M-pole system which is represented by the impulse response

$$x(t) = \sum_{m=1}^{M} a_m e^{\bar{s}_m t} \tag{1}$$

where $\{\bar{s}_m\}$ are complex poles and $\{a_m\}$ the corresponding residues. The system transfer function is then obtained by taking the Laplace Transform of x(t), which yields

$$\bar{X}(s) = \sum_{m=1}^{M} \frac{a_m}{s-\bar{s}_m} \tag{2}$$

If x(t) is uniformly sampled at $t_n=nT$, n=0,1,...,N-1, then, instead of the Laplace Transform, the z-transform is applied:

$$X(z) = \sum_{n=0}^{N-1} x_n z^{-n} \tag{3}$$

where $x_n=x(t_n)$ and $z=e^{st}$. The z-transform of $\{x_n\}$ is representative of the Laplace transform of x(t). From Eq. (2) it is seen that $\bar{X}(s)$ has singularity at the poles $\{\bar{s}_m\}$. Similarly, the z-transform X(z) tends to have peak values at $z_m = e^{\bar{s}_m T}$. Thus by evaluating X(z) along a contour near the poles one can estimate the pole locations. if X(z) is evaluated at the set of equally spaced points around the unit circle, $z_k = e^{-j2\pi k/N}$, k=0, 1, 2, ..., N-1, it results in a discrete Fourier Transform (DFT):

$$X(z_k) = \sum_{n=0}^{N-1} x_n e^{-j2\pi nk/N} \qquad k=0,\ 1,\ \ldots,\ N-1 \tag{4}$$

By employing the FFT algorithm. $X(z_k)$ can be computed efficiently. To achieve this efficiency, N is required to be a highly composite number. If one is to employ a power-of-2 FFT algorithm, this can be accomplished by augmenting the N-point sequences $\{x_n\}$ with a sufficient number of zeros so that their total length is a power of 2.

The DFT is effective in locating the poles only if the poles are on or near the jw axis. In order to locate a pole which is away from the jw axis, one would need to compute the z-transform along a general contour. There are two general approaches to this problem: (a) the contour is a circle that is concentric with the unit circle, and (b) the contour is a spiral. The former is called modified FFT and the latter is called chirp z-transform (CZT)

(A) Modified FFT

A concentric circle on the z-plane is equivalent to a straight line on the s-plane. The correspondence is shown in Figure 1. Let $\{s_k\}$ and $\{z_k\}$ be the corresponding points on the s-plane and z-plane, respectively. Let $f_s = 1/T$ be the sampling frequency. Then $s_k = \sigma_o + jw_k$, where $w_k = 2\pi k f_s/N$. The $\{z_k\}$ are then given by

$$z_k = e^{\sigma_o T} e^{j2\pi k/N} \quad k=0, 1, 2, \ldots, N-1. \tag{5}$$

where $|z_k| = e^{\sigma_o T}$ is the radius of the circle. Eq. (4) can now be written as

$$X(z_k) = \sum_{n=0}^{N-1} (x_n e^{-n\sigma_o T}) e^{-j2\pi nk/N} \tag{6}$$

Eq. (6) shows that, to evaluate X(z) along the contour $|z| = e^{\sigma_o T}$ on the z-plane or along the straight vertical line $\sigma=\sigma_o$ on the s-plane, one can multiply the sequence $\{x_n\}$ by $\{e^{-n\sigma_o T}\}$ and then take the FFT. If one is interested in obtaining frequency samples equally spaced over a small portion of the unit circle, one may augment the original sequence with zeros, take the FFT, and retain the frequency samples of interest. For example, if, instead of the frequency spacing F = 1/NT, one desires to have a smaller spacing F' = 1/LT, one has to augment L-N zeros to

x_n. Namely, let

$$\hat{x}_n = \begin{cases} x_n & n=0, 1, \ldots, N-1 \\ 0 & n=N, N+1, \ldots, L-1 \end{cases} \tag{7}$$

and then evaluate the following equations by the FFT.

$$X(z_k) = \sum_{n=0}^{L-1} (\hat{x}_n e^{-\sigma_o nT}) e^{j2\pi kn/L} \quad k=0, 1, 2, \ldots, L-1. \tag{8}$$

From the L frequency samples one then retains only the desired spectral points.

(B) CZT

To evaluate Eq. (3) along the contour as shown in Fig. 2, let

$$s_k = s_o + k\Delta s \qquad k=0, 1, \ldots, J-1 \tag{9}$$

where $\Delta s = \Delta\sigma + j\Delta w$, $\Delta\sigma$ is the increment along σ-axis and Δw is the increment along the jw-axis. In the z-plane, the contour is a spiral given by

$$z_k = e^{s_o T} e^{k\Delta s T} \quad k=0, 1, \ldots, J-1 \tag{10}$$

which has a radius of $|z_k| = e^{(\sigma_o + k\Delta\sigma)T}$ and a uniform angle of increment $\Delta\theta = T\Delta w$. Eq. (3) can now be written as

$$X(z_k) = \sum_{n=0}^{N-1} x_n e^{-ns_o T} e^{-nkT\Delta s} \quad k=0, 1, \ldots, J-1 \tag{11}$$

By using the Bluestein's identity

$$nk = \tfrac{1}{2}[n^2 + k^2 - (k-n)^2] \tag{12}$$

one can write Eq. (11) as

$$X(z_k) = e^{-k^2 T\Delta s/2} \sum_{n=0}^{N-1} g_n h_{k-n} \tag{13}$$

where $g_n = x_n e^{-ns_o T} e^{-n^2 T\Delta s/2}$ (14)

and

$$h_n = e^{-n^2 T\Delta s/2} \tag{15}$$

Eq. (13) shows that the CZT can be evaluated by high-speed convolution with the use of the FFT altorithm.

III The Tseng Window

Since the data sequence is finite, both the modified FFT and CZT suffer from the leakage effects. The main impediment of the leakage effects is the high near-sidelobes of the spectral window. In detecting a small pole in the presence of nearby strong poles on the jw axis, the Tseng window has been shown to be effective [7]. Thus a special Tseng window designed to have low near-sidelobes will be employed to improve the detectability of the CZT.

Consider a data window specified by a set of 2K weights $\{w_0, w_1, w_2, \ldots, w_{2K-1}\}$. The spectral window is related to the data window by the Fourier Transform:

$$W(f) = \sum_{k=0}^{2K-1} w_k e^{-j2\pi fkT} \tag{16}$$

By assuming that the data window is real and even, Eq. (16) can be written as

$$W(f) = 2e^{-j(2K-1)\pi fT} x \prod_{k=1}^{K-1} (x^2-\gamma_k^2) \Big|_{x=\cos\pi fT} \tag{17}$$

where $\{\gamma_k\}$ are the zeros of the polynomial. By controlling the locations of the zeros one can form a spectral window with a desired sidelobe structure. To suppress near-sidelobes the zeros $\{\gamma_k\}$ can be chosen as follows:

$$\gamma_k = \cos\left(\frac{\pi}{2K} z_k\right) \qquad k=1, 2, \ldots, K-1 \tag{18}$$

where

$$z_k = k \quad \text{for } k \geq k_o \tag{19}$$

and

$$z_{k-1} = z_k - \Delta_k \quad \text{for } 1 \leq k \leq k_o \tag{20}$$

with

$$\Delta_k = 1 - A\sin\left[\left(\frac{k_o-k}{k_o-1}\right)\frac{\pi}{2}\right] \qquad (21)$$

In Eqs. (20) and (21), Δ_k is the increment of $\{z_k\}$, k_o is the number of the near-sidelobes to be suppressed, and A is a parameter to control the near-sidelobe level ($A \leq 1$). The design principle is based on the observation that to suppress the first k_o sidelobes the zeros $\{\gamma_k\}$ should have small spacings, which is achieved by making the increments $\{\Delta_k\}$ small. The smallest increment occurs at k=1 and is given by $\Delta_1 = 1 - A$. By increasing A and/or k_o the near-sidelobe level can be reduced to any desired value.

A Tseng window is designed to suppress the near-sidelobes for 128 uniformly sampled weightings. The chosen parameters are: k_o=4 and A=0.7. Fig. 3 shows the rectangular and the Tseng windows. The rectangular window is obtained by setting A=0. It is seen that as A is increased from 0 to 0.7 the near-sidelobes are effectively reduced from -13dB to -47dB.

IV. Enhancement of Poles

The chirp z-transform algorithm and the Tseng window are now applied to a four-pole system. Attention is focused on the resolvability of two closely spaced poles which have large amplitude differences. The impulse response of the four-pole system is represented by Eq. (1) with the following parameters:

a_1=0.1, σ_1=-250Hz, f_1=1000Hz

a_2=1.0, σ_2=-300Hz, f_2=1250Hz

a_3=1.0, σ_3=-150Hz, f_3=2000Hz

a_4=0.1, σ_4=-200Hz, f_4=2250Hz

The sampling frequency is chosen as 10kHz. There are 128 samples. These samples are weighted by 128 weightings of the Tseng data window. The chirp z-transform of these samples was then evaluated along eight contours, which are shown in Fig. 4 along with the s-plane pole location. The first contour is on the jw axis; this is the regular FFT. The rest of the contours are parallel to the jw axis with σ_o=-50, -100, -150, -200, -250, -300 and -350 Hz, respectively. These are called modified FFT and are special cases of CZT. The spectra of the four-pole system along these contours are presented in Figs.5 through 11. Both the spectra using the rectangular and the Tseng windows, respectively, are shown for comparison. Fig. 5 (for σ_o=0) shows that the FFT can detect the frequencies at f_2 (1250 Hz) and f_3 (2000 Hz) only. Both windows fail to detect the two small poles at f_1 (1000 Hz) and f_4 (2250 Hz). As the contour moves to σ_o=-50 Hz Fig. 6 indicates that, even though the Tseng window shows sharper resolution, both windows still could not detect the two small poles. As the contour is moved further to the left at σ_o=-100 Hz, Fg. 7 shows a deep valley between f_2 (1250 Hz) and f_3 (2000 Hz). The Tseng window shows a small peak at f_4 (2250 Hz) but the rectangular window still could not detect the two small poles. Now as the contour is moved to σ_o=-150 Hz, which passes right through the pole at f_3 (2000 Hz), the Tseng window can now clearly detect and resolve the pole at f_4 (σ_4=-200 Hz and f_4=2250 Hz), as shown in Fig. 8. In order to detect the small pole at f_1 = 1000 Hz the contour is moved further to the left at σ_o=-200 Hz. The Tseng window now starts indicating the pole at f_1 (σ_1=-250 Hz) (see Fig. 9). By further moving the contour to the left at σ_o=-250 Hz, which passes through the pole at f_1, the results in Fig. 10 indicate that the Tseng window can detect all the poles while the

rectangular window still can not detect the two small poles. As the contours are pushed further to the left, σ_o=-300 Hz and σ_o=-350 Hz in Fig. 11 and 12 respectively, the resolution at each pole becomes sharper, the peaks at f_1, f_2 and f_4, however, suffer from splitting. This is due to the computation noise as seen from Eq. (6) where x_n is multiplied by $e^{-n\sigma_o T}$ which can become very large when $-n\sigma_o$ becomes large. From these spectra it appears that the best contour is the one at σ_o=-250 Hz, which lies closest to the smallest pole at f_1. In all these examples the rectangular window never detected the two small poles, while by properly choosing the contour the Tseng window is capable of detecting the two small poles.

In the next example, instead of the modified FFT, the regular CZT is applied to the samples along four tilted contours. Fig 13 shows the s-plane pole locations and the four contours on the s-plane. For each contour the rectangular and the Tseng windows are applied separately. The results are presented in Figs. 14 through 17. Fig. 14 shows the spectra along the contour $\Delta\sigma$=1. It is seen that the Tseng window shows sharper resolution. Both windows could detect the larger poles at f_2 (1250 Hz) and f_3 (2000 Hz) but both failed to detect the small poles. As the contour is tilted more to $\Delta\sigma$=2, which passes between the poles at f_3 and f_4, the CZT results show that the Tseng window has better resolution (see Fig. 15): The pole at f_4 is clearly resolved. But the rectangular window again fails to detect the two small poles. In order to detect the small pole at f_1 (1000 Hz) the contour is further tilted to $\Delta\sigma$=3. The results are presented in Fig. 16. The resolution of the Tseng window is now very sharp at f_3 and f_4 (2250 Hz) but failed to detect the small pole at f_1. Instead, the high frequency noise starts

distorting the spectrum peak at f_4. If the contour is now further tilted to $\Delta\sigma=4$, the high frequency noise becomes worse and the small pole at f_1 still is not resolved (see Fig. 17). In all four contours evaluated the rectangular window never detected the two small poles.

The two examples demonstrated the effectiveness of the CZT and the Tseng window in detecting and resolving a small pole located far away from the jw axis. The examples also illustrated the importance of choosing an appropriate contour. The main limitation of the new technique is the high frequency computational noise. How to cope with this problem is currently being studied. Further research along this line will be reported in the future.

V. Conclusion

A new technique for detecting a small pole in the presence of a nearby strong pole is presented in this paper. By simultaneously applying the CZT and Tseng window, the new technique is shown to be able to detect and resolve a small pole. Numerous spectra are plotted for a four-pole system along various contours. These examples demonstrated the effectiveness of the Tseng window as compared to the rectangular window in detecting and resolving a small pole located far away from the jw axis. These examples also illustrated the importance of choosing an appropriate contour in detecting the poles.

References

[1] C.E. Baum, "Emerging Technology for Transient and Broad-Band Analysis and Synthesis of Antennas and Scatterers," Proc. IEEE, Vol. 64, No. 11, pp. 1598-1616, Nov. 1976.

[2] D.L. Moffatt and R.K. Mains, "Detection and Discrimination of Radar Targets," IEEE Trans. Antennas Propagat., Vol 23, No. 3, pp. 358-367, May, 1975.

[3] M.L. Van Blaricum and R. Mittra, "Problems and Solutions Associated with Prony's Method for Processing Transient Data," IEEE Trans. Antennas Propagat., Vol 26, No. 1, pp. 174-182, Jan. 1978.

[4] V.K. Jain, T.K. Sarkar, D.D. Weiner, "Extension of Pencil-of-Function Method to Reverse-Time Processing with First-Order Digital Filters" TR-80-4, Contract N00014-79-C-0598, Aug. 1980.

[5] M.L. Van Blaricum, "Difficulties Present in Algorithms for Determining the Rank and Proper Poles with Prony's Method," 1979 RADC Spectrum Estimation Workshop, pp. 147-155, Oct. 1979.

[6] L.R. Rabiner, R.W. Schafer, and C.M. Rader, "The Chirp z-Transform Algorithm and Its Application," The Bell System Technical Journal, May-June 1969.

[7] F.I. Tseng, T.K. Sarkar and D.D. Weiner, "A Novel Window for Harmonic Analysis." To be published in the IEEE Transactions on Acoustics, Speech and Signal Processing.

Fig. 1. The correspondence of a z-plane contour to an s-plane contour ($z=e^{sT}$, $r_o=e^{\sigma_o T}$).

Fig. 2. The correspondence of a z-plane contour to an s-plane contour for the CZT.

Fig. 3. The spectral windows of the rectangular (dash) and the Tseng (solid) weightings.

Fig. 4. The s-plane locations of the poles and the eight contours for evaluation of the modified FFT.

Fig. 5. Detection of a four-pole signal by FFT with the rectangular (dash) and the Tseng (solid) windows ($\sigma_o=0$)

Fig. 6. Detection of a four-pole signal by modified FFT with the rectangular (dash) and the Tseng (solid) windows ($\sigma_o=-50Hz$)

Fig. 7. Detection of a four-pole signal by modified FFT with the rectangular (dash) and Tseng (solid) windows. ($\sigma_o=-100Hz$).

Fig. 8. Detection of a four-pole signal by modified FFT with the rectangular (dash) and Tseng (solid) windows. ($\sigma_o=-150Hz$).

Fig. 9. Detection of a four-pole signal by modified FFT with the rectangular (dash) and Tseng (solid) windows ($\sigma_o=-200Hz$).

Fig. 10. Detection of a four-pole signal by modified FFT with the rectangular (dash) and Tseng (solid) windows. ($\sigma_o=-250Hz$).

Fig.11. Detection of a four-pole signal my modified FFT with the rectangular (dash) and Tseng (solid) windows ($\sigma_o=-300Hz$).

Fig. 12. Detection of a four-pole signal by modified FFT with the rectangular (dash) and Tseng (solid) windows ($\sigma_o=-350Hz$).

Fig.13. The s-plane locations of the poles and the four contours for evaluation of the CZT.

Fig. 14. Detection of a four-pole signal by the CZT with the rectangular (dash) and Tseng (solid) windows ($\Delta\sigma=1$).

Fig. 15. Detection of a four-pole signal by the CZT with the rectangular (dash) and Tseng (solid) windows. ($\Delta\sigma$=2).

Fig. 16. Detection of a four-pole signal by the CZT with the rectangular (dash) and Tseng (solid) windows. ($\Delta\sigma$=3).

Fig. 17. Detection of a four-pole signal by the CZT with the rectangular (dash) and Tseng (solid) windows ($\Delta\sigma$=4).

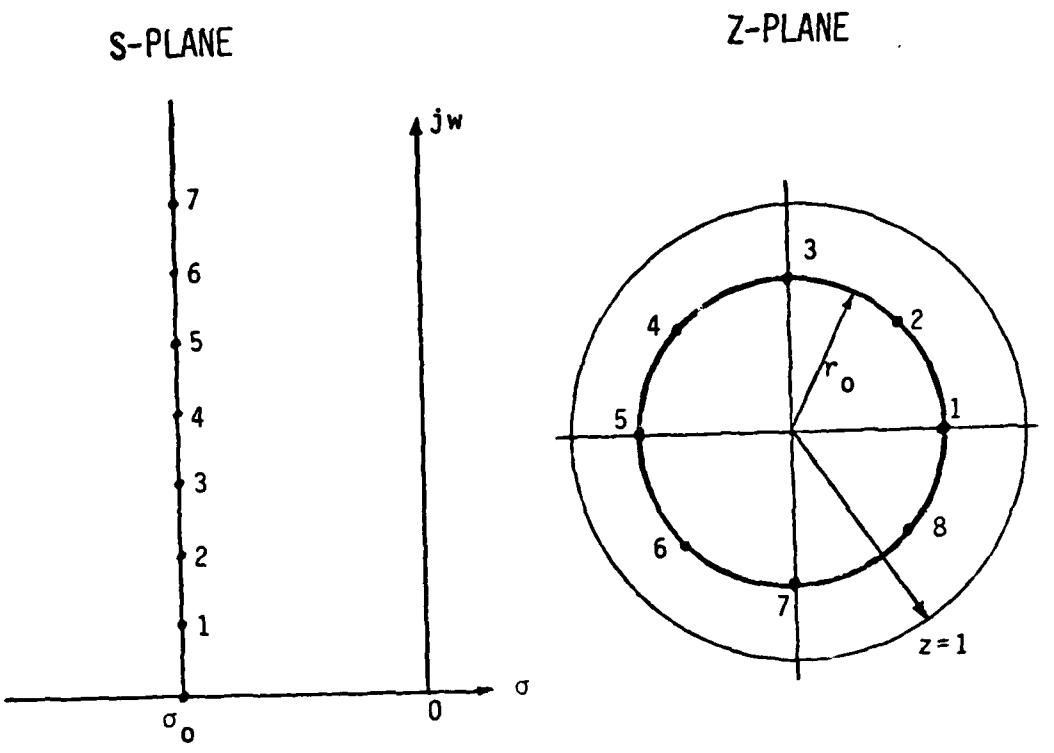

FIG. 1

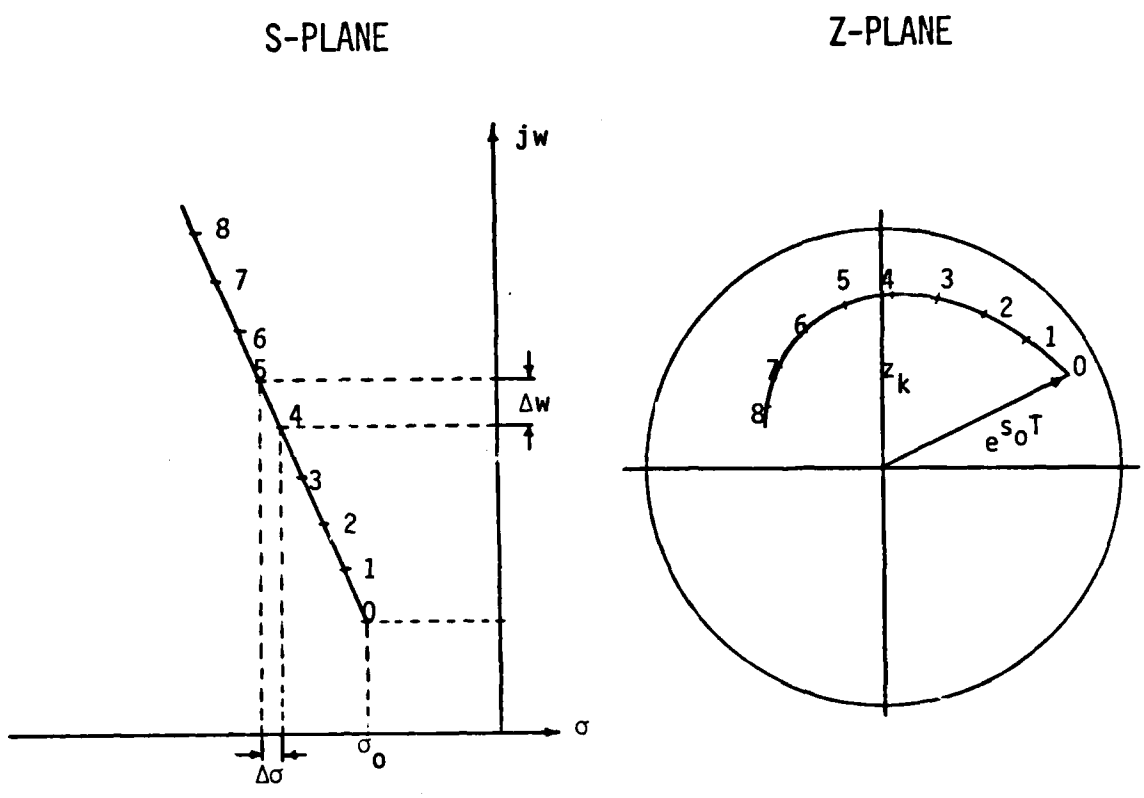

FIG. 2

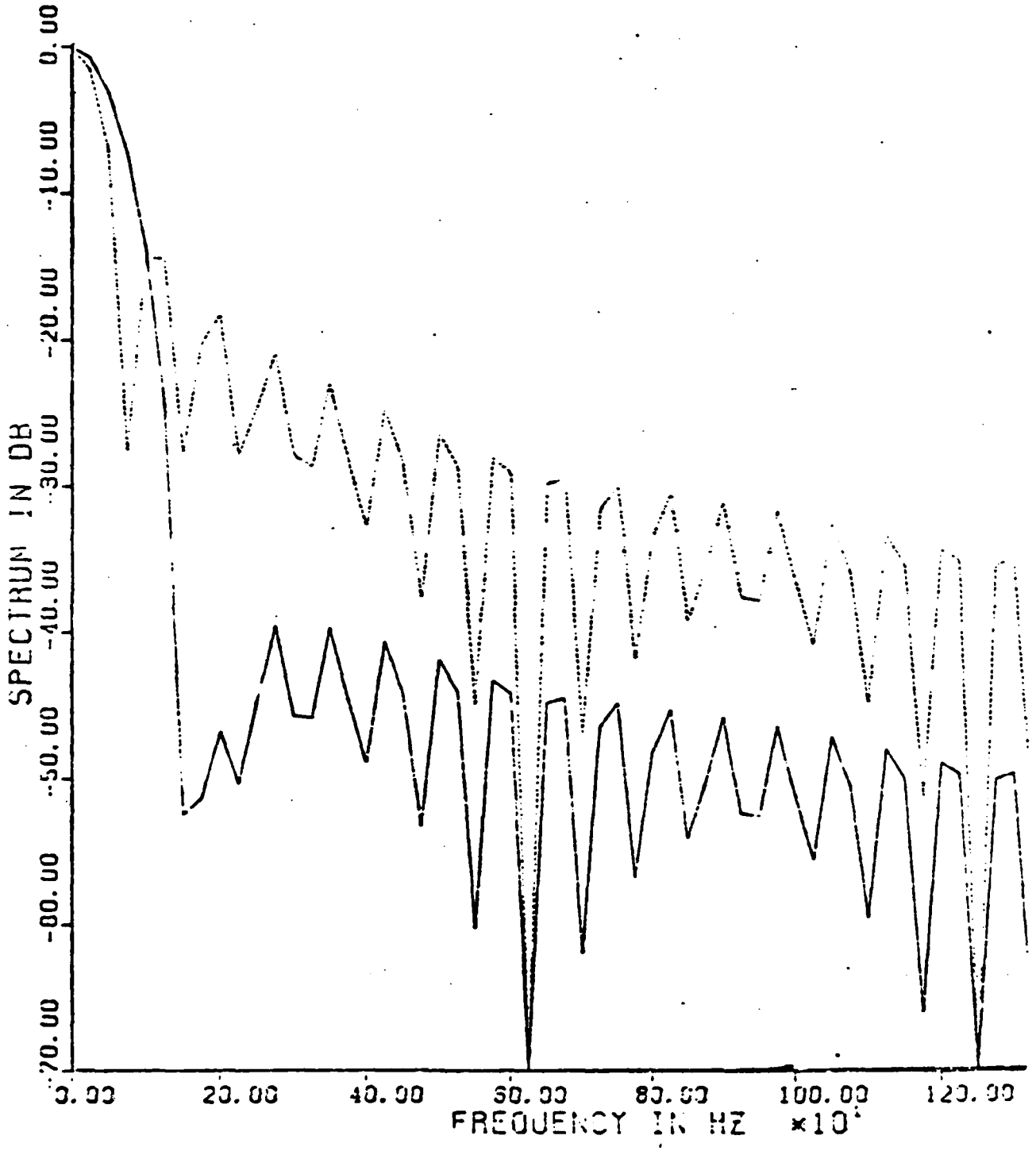
SPECTRUM IN DB
0.00
-10.00
-20.00
-30.00
-40.00
-50.00
-60.00
-70.00
0.00
20.00
40.00
60.00
80.00
100.00
120.00
FREQUENCY IN HZ ×10³

FIG. 3

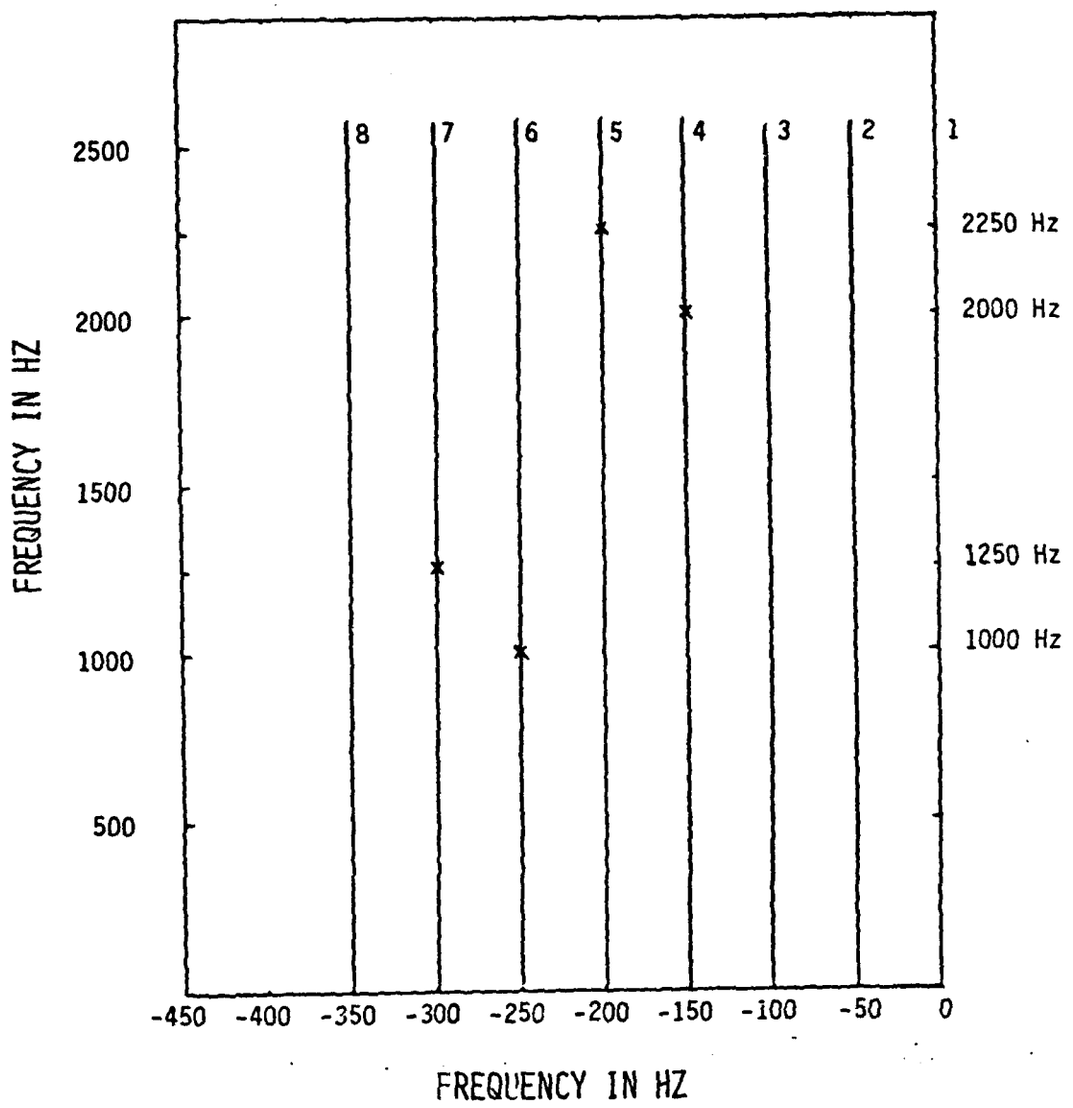
8
7
6
5
4
3
2
1
2500
2000
1500
1000
500
2250 Hz
2000 Hz
1250 Hz
1000 Hz
FREQUENCY IN HZ
-450
-400
-350
-300
-250
-200
-150
-100
-50
0
FREQUENCY IN HZ

FIG. 4

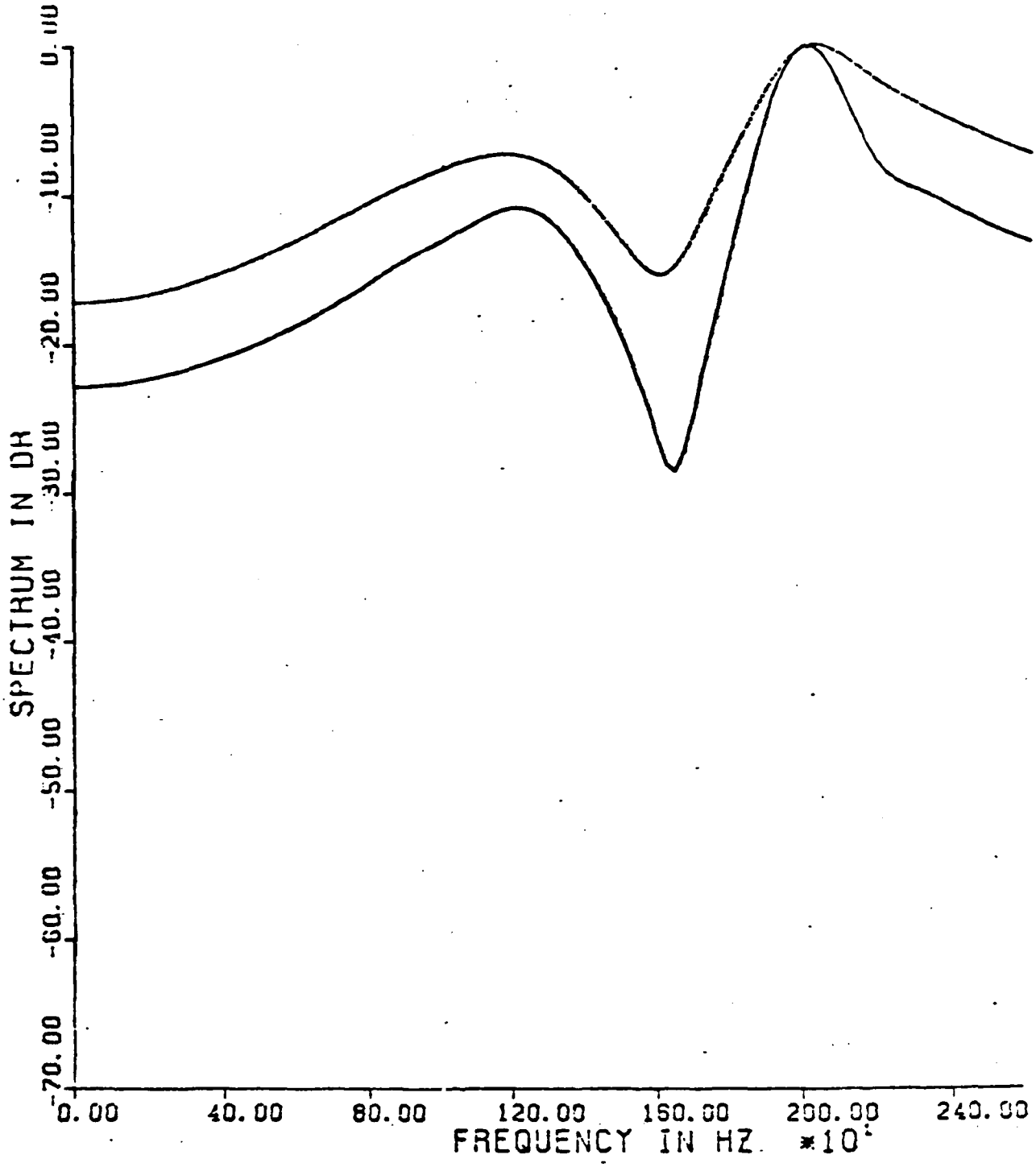
SPECTRUM IN DH
0.00
-10.00
-20.00
-30.00
-40.00
-50.00
-60.00
-70.00
0.00
40.00
80.00
120.00
160.00
200.00
240.00
FREQUENCY IN HZ. *10²

FIG. 5

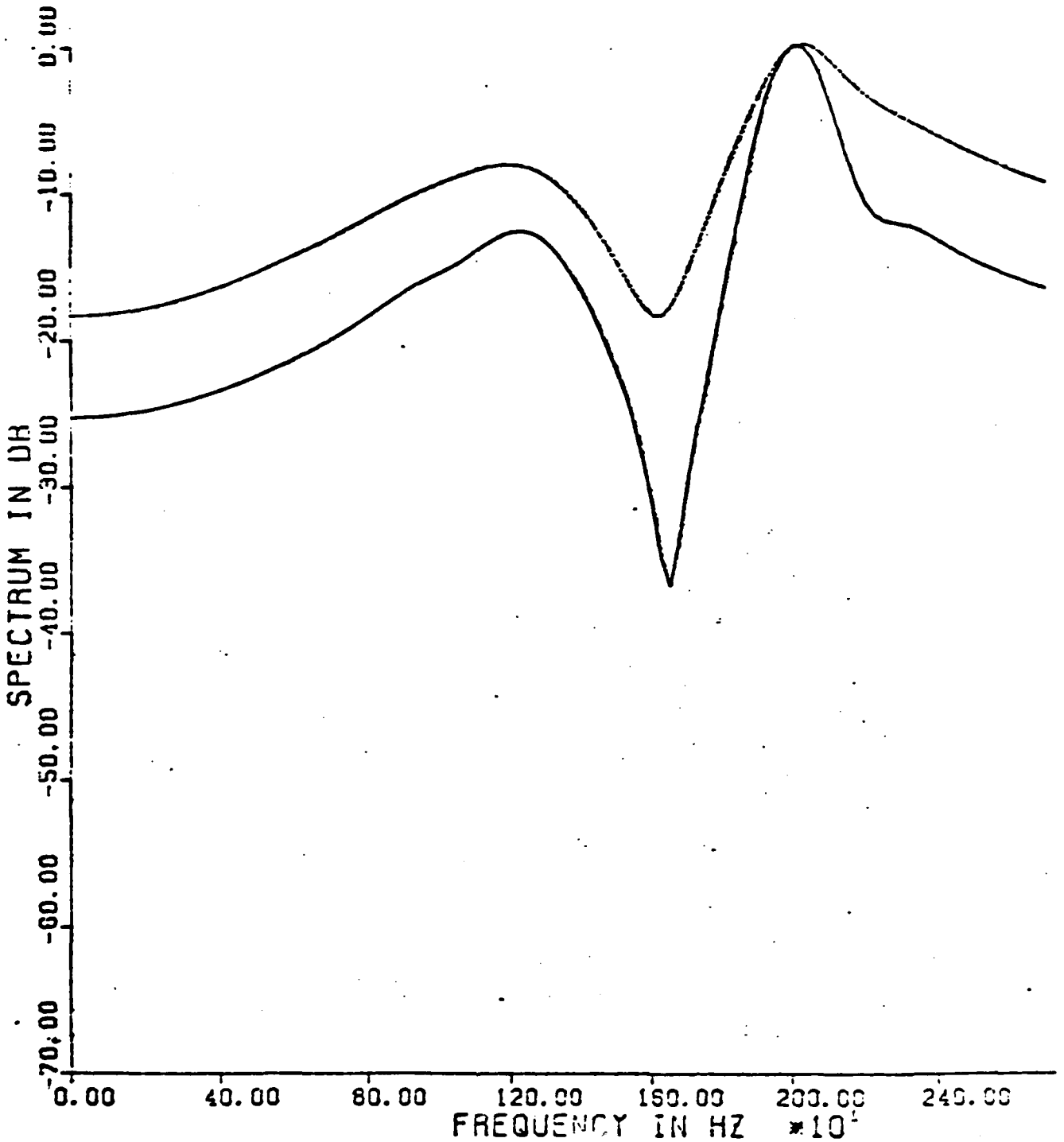
0.00
-10.00
-20.00
-30.00
-40.00
-50.00
-60.00
-70.00
SPECTRUM IN DB
0.00
40.00
80.00
120.00
160.00
200.00
240.00
FREQUENCY IN HZ *10

FIG. 6

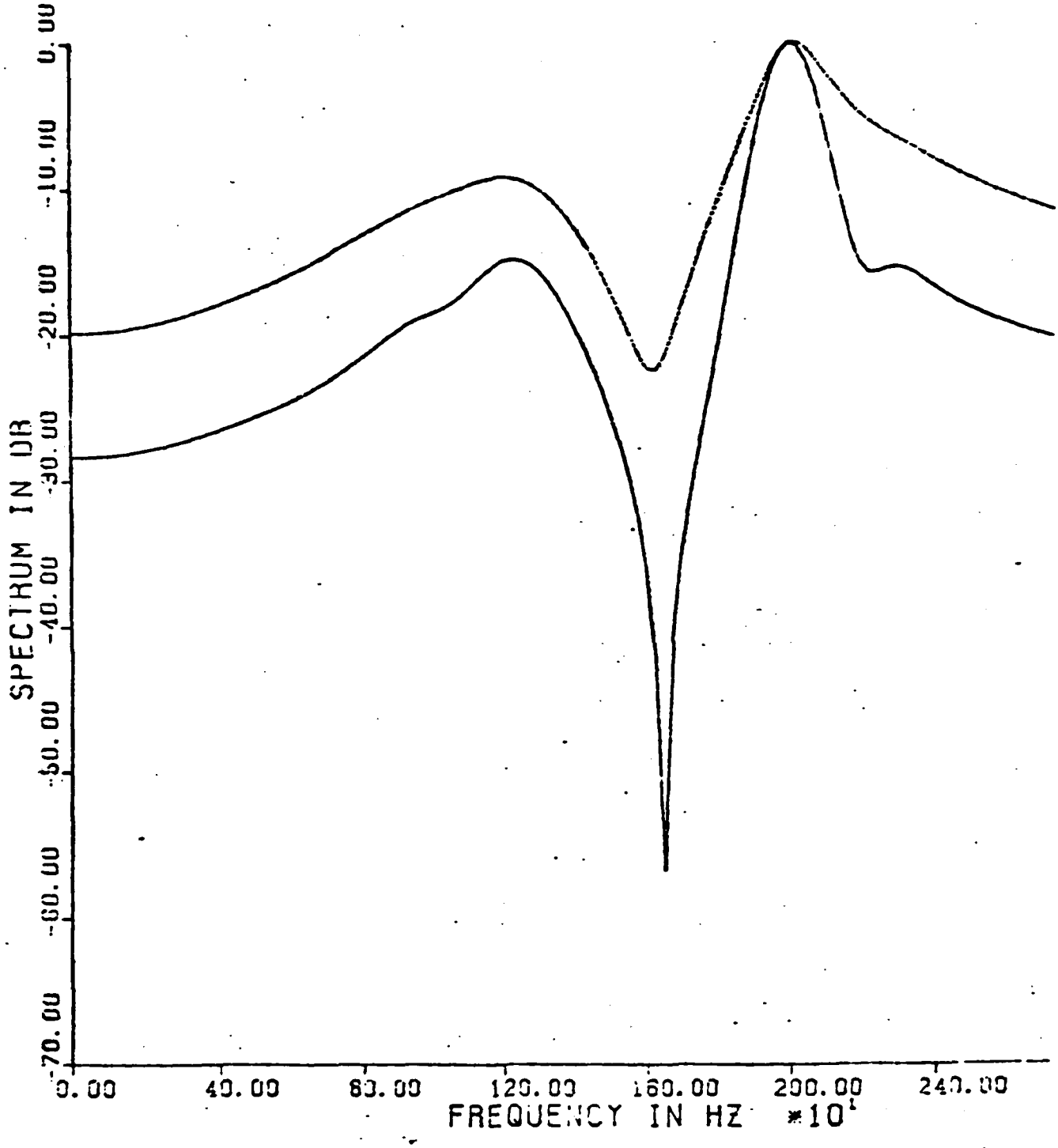
0.00
-10.00
-20.00
-30.00
-40.00
-50.00
-60.00
-70.00
SPECTRUM IN DB
0.00
40.00
80.00
120.00
160.00
200.00
240.00
FREQUENCY IN HZ *10¹

FIG. 7

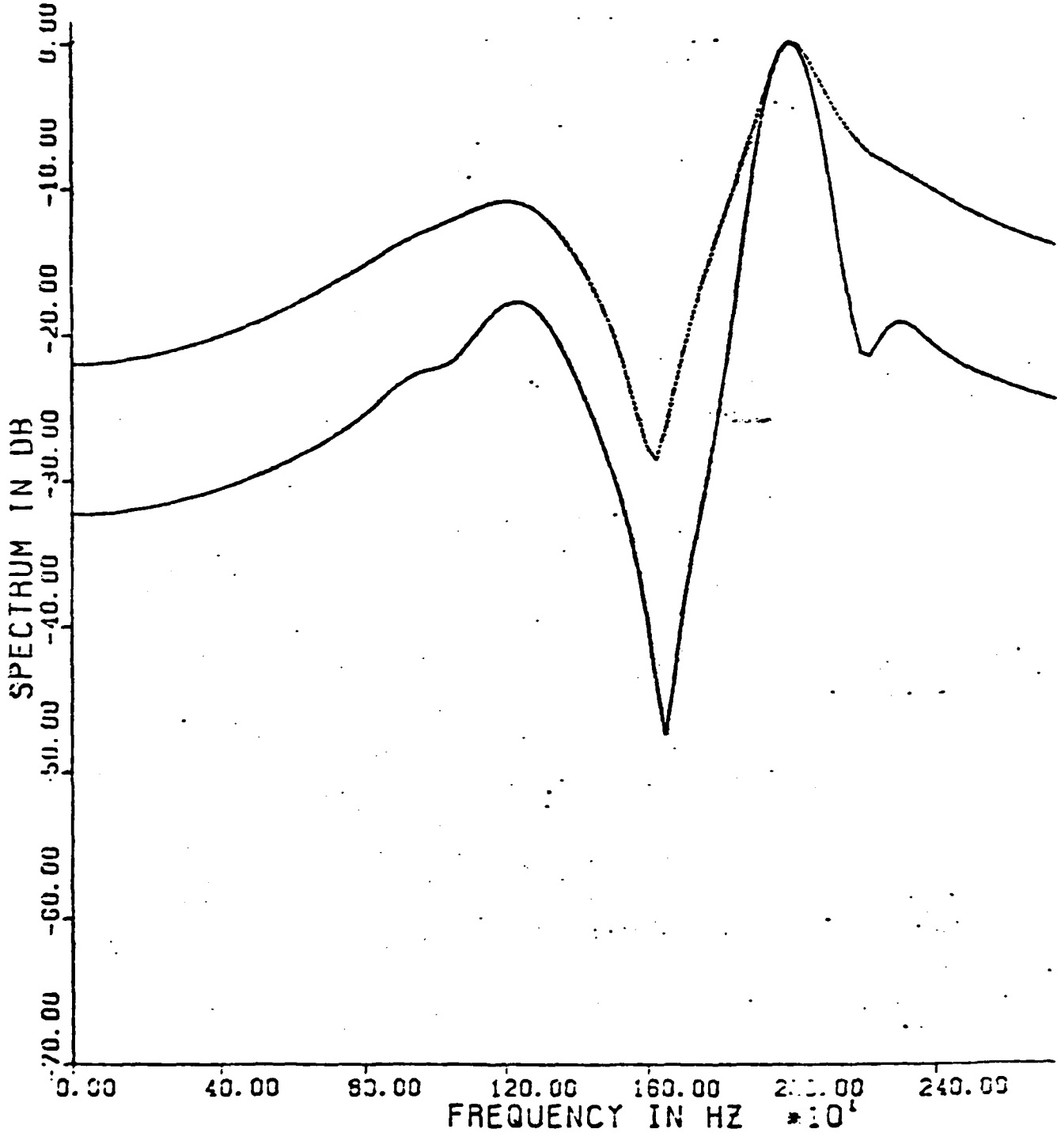
SPECTRUM IN DB
0.00
-10.00
-20.00
-30.00
-40.00
-50.00
-60.00
-70.00
0.00
40.00
80.00
120.00
160.00
200.00
240.00
FREQUENCY IN HZ *10¹

FIG. 8

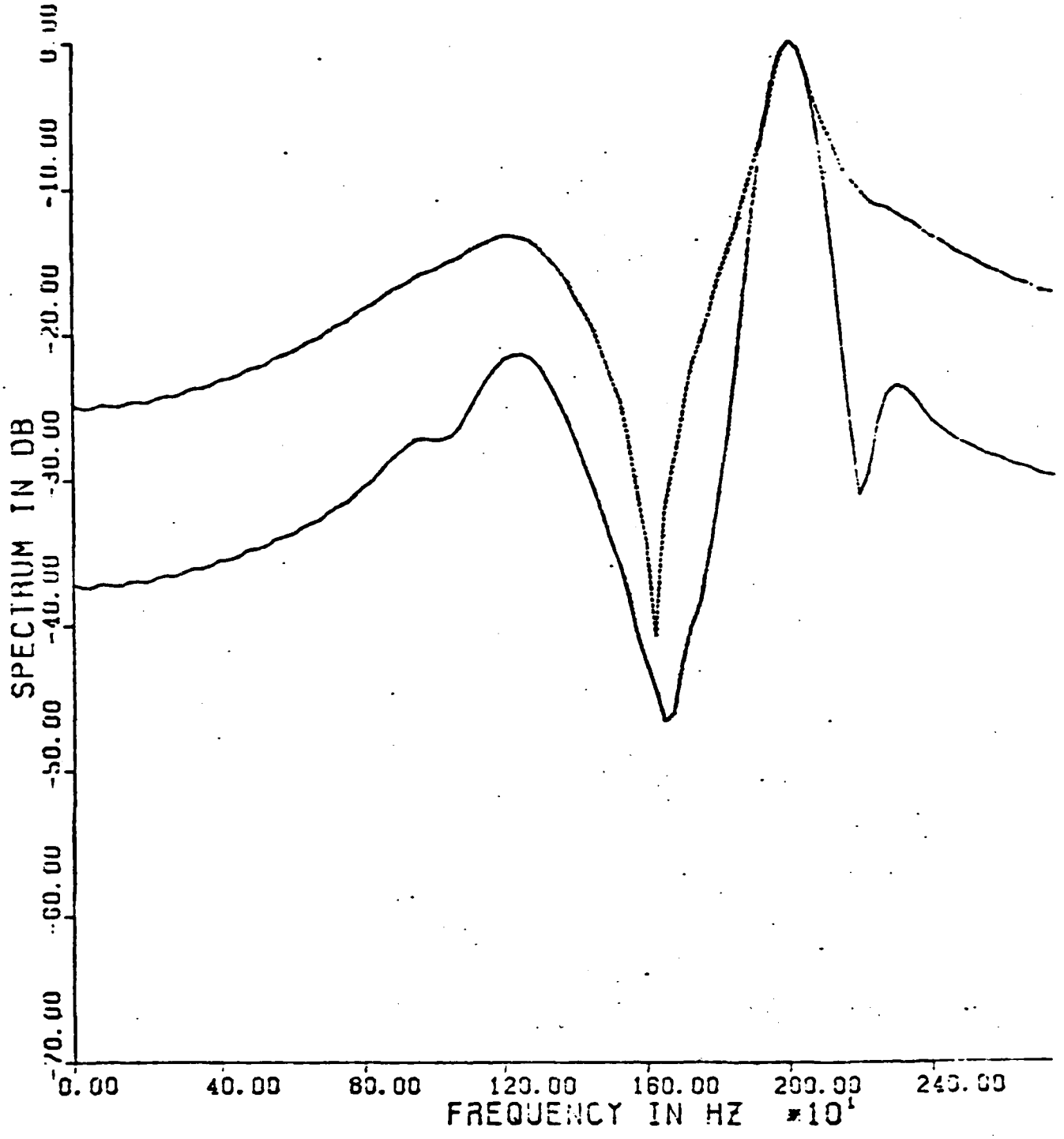
SPECTRUM IN DB
0.00
-10.00
-20.00
-30.00
-40.00
-50.00
-60.00
-70.00
0.00
40.00
80.00
120.00
160.00
200.00
240.00
FREQUENCY IN HZ *10¹

FIG. 9

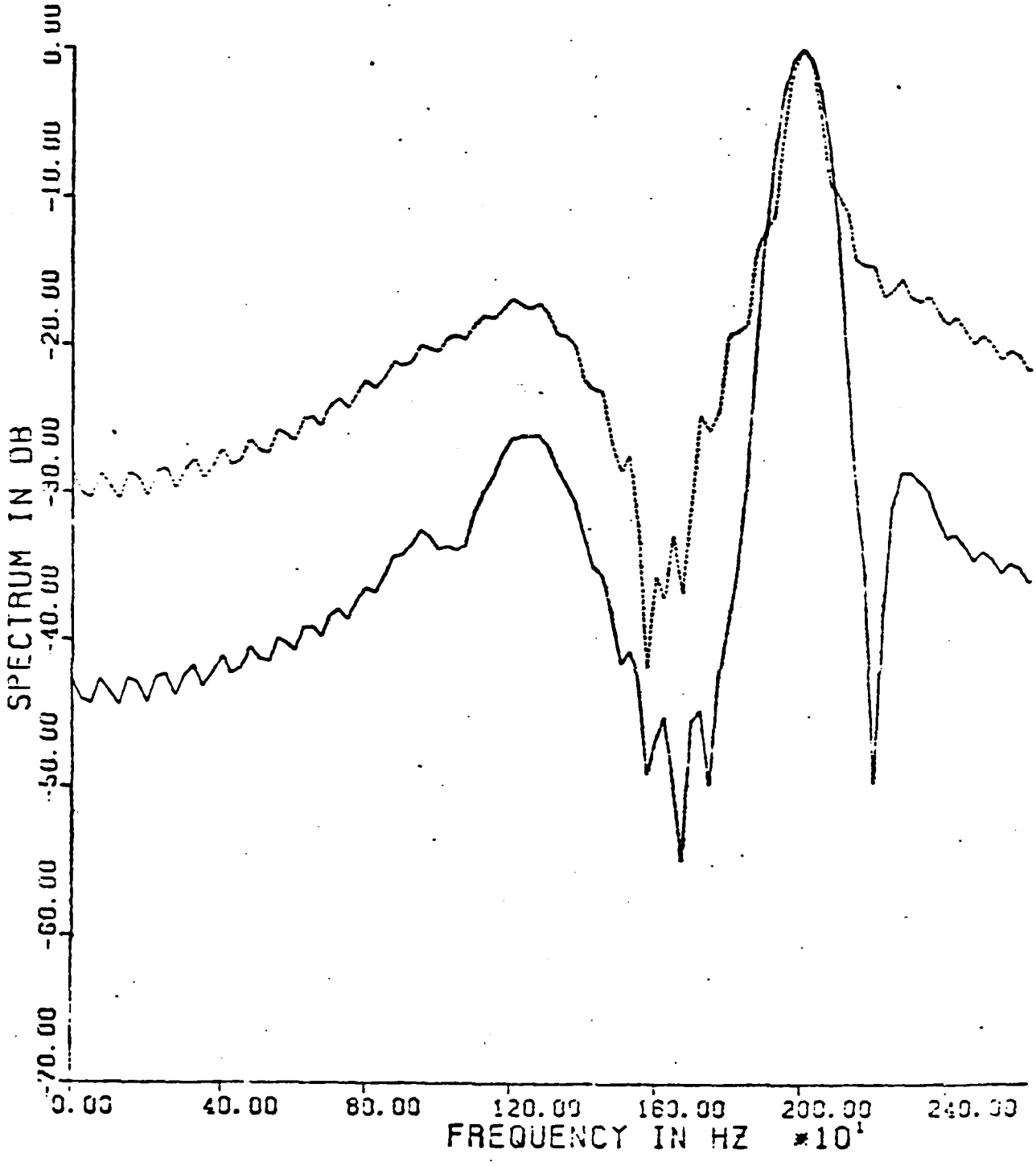
SPECTRUM IN DB
0.00
-10.00
-20.00
-30.00
-40.00
-50.00
-60.00
-70.00
0.00
40.00
80.00
120.00
160.00
200.00
240.00
FREQUENCY IN HZ *10¹

FIG 10

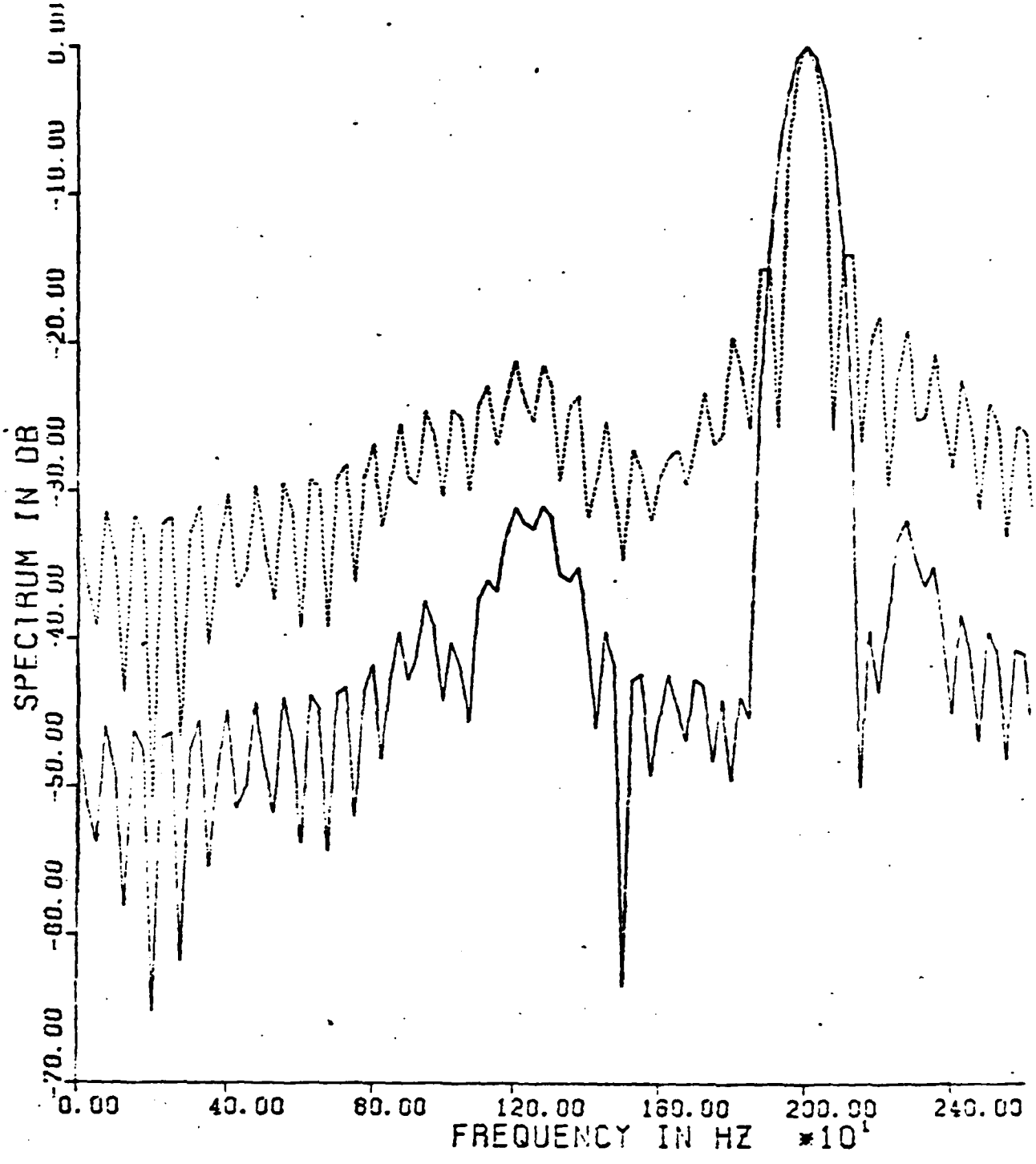
SPECTRUM IN DB
0.00
-10.00
-20.00
-30.00
-40.00
-50.00
-60.00
-70.00
0.00
40.00
80.00
120.00
160.00
200.00
240.00
FREQUENCY IN HZ *10¹

FIG. 11

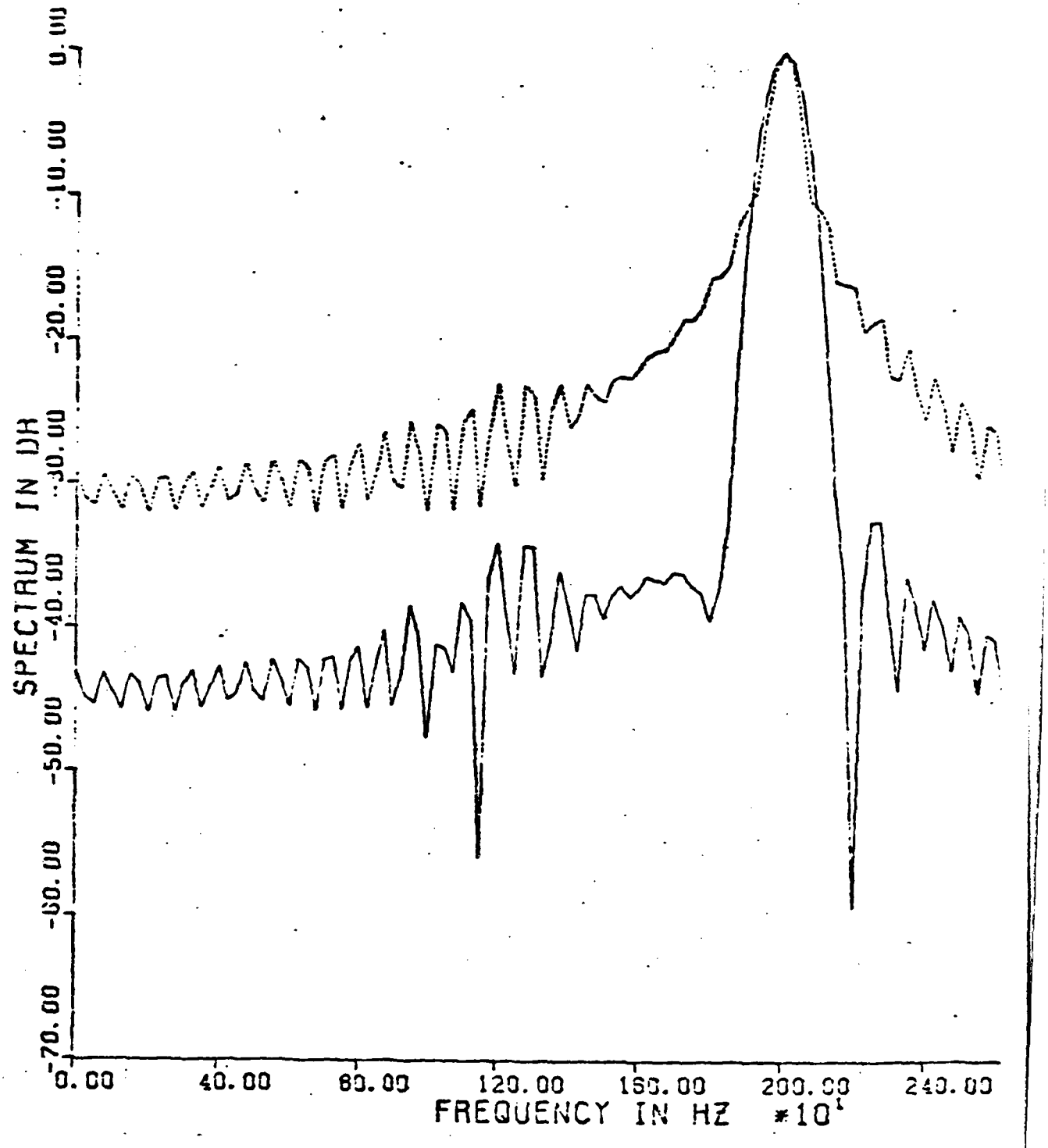
SPECTRUM IN DB
0.00
-10.00
-20.00
-30.00
-40.00
-50.00
-60.00
-70.00
0.00
40.00
80.00
120.00
160.00
200.00
240.00
FREQUENCY IN HZ *10¹

FIG. 12

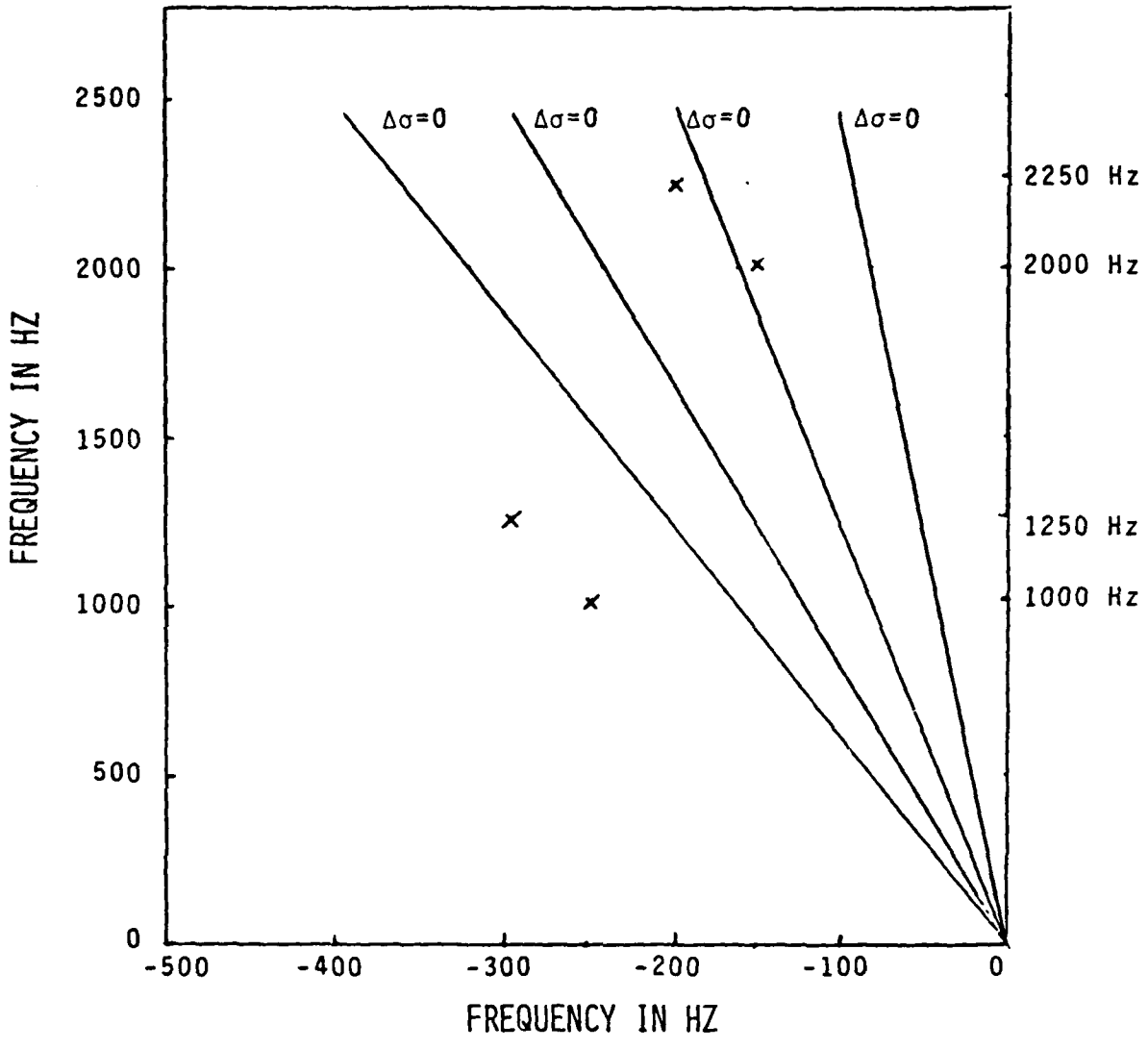
2500
2000
1500
1000
500
0
FREQUENCY IN HZ
Δσ=0
Δσ=0
Δσ=0
Δσ=0
2250 Hz
2000 Hz
1250 Hz
1000 Hz
-500
-400
-300
-200
-100
0
FREQUENCY IN HZ

FIG.13

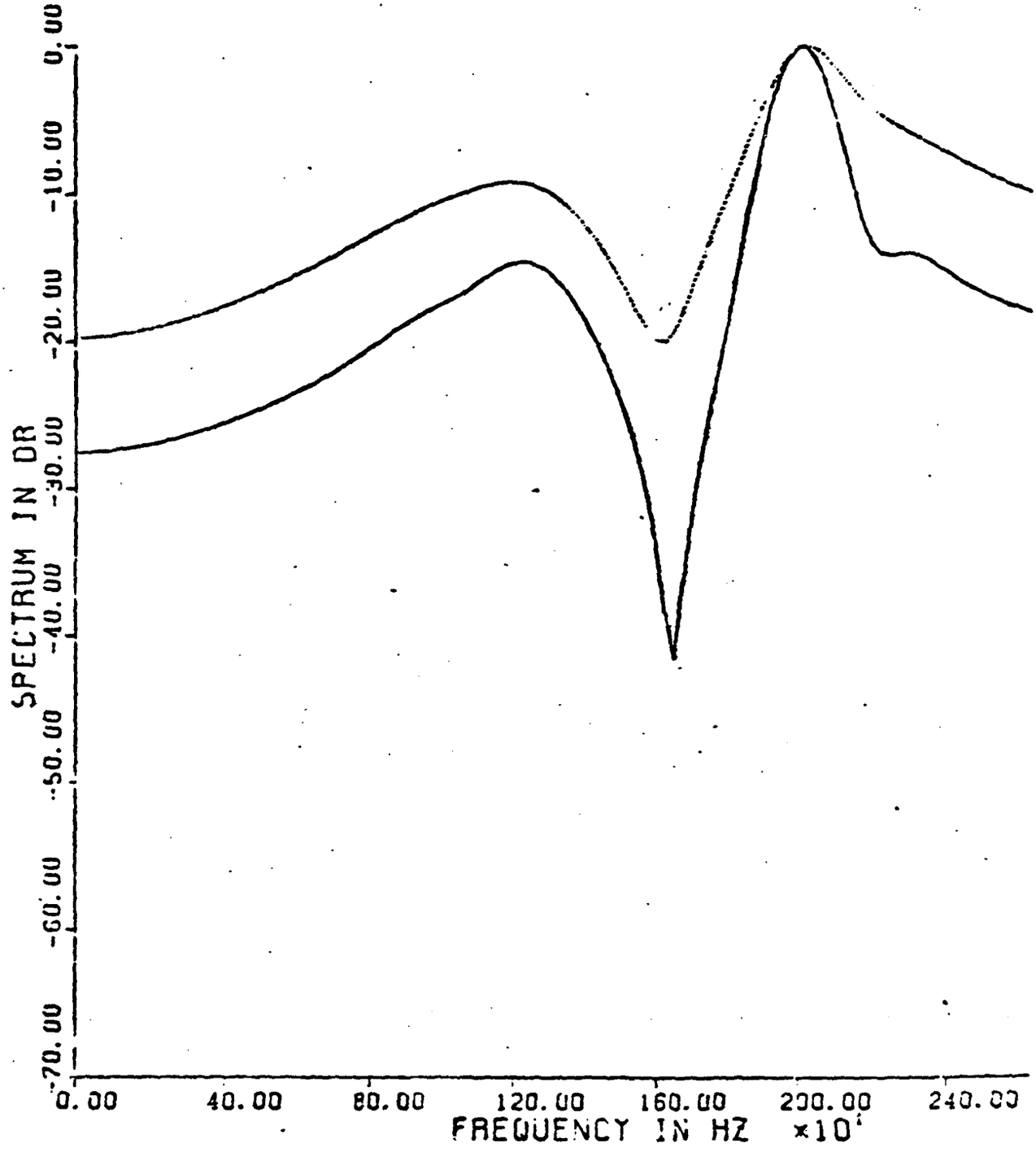
0.00
-10.00
-20.00
-30.00
-40.00
-50.00
-60.00
-70.00
SPECTRUM IN DR
0.00
40.00
80.00
120.00
160.00
200.00
240.00
FREQUENCY IN HZ ×10²

FIG. 14

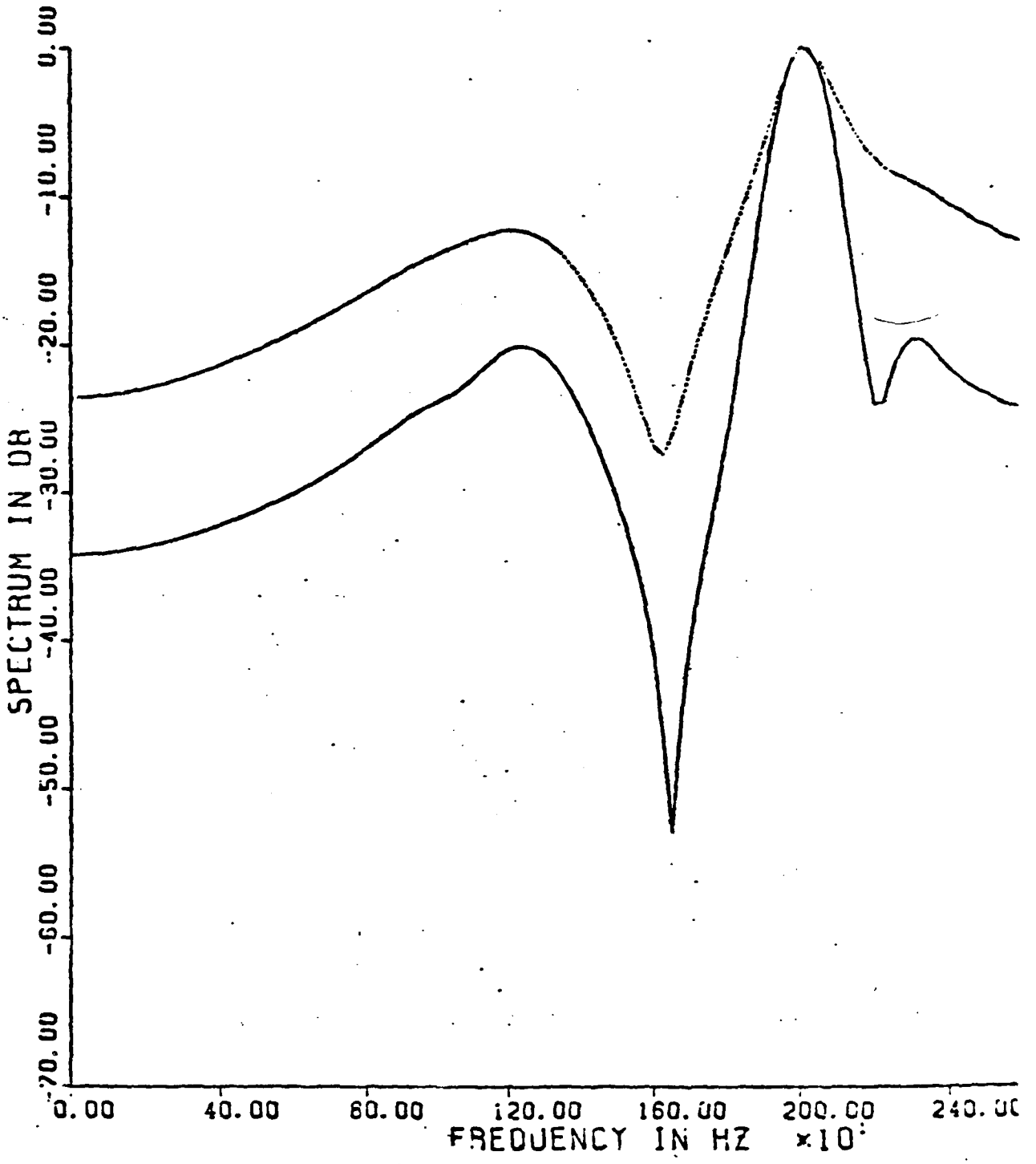
SPECTRUM IN DB
0.00
-10.00
-20.00
-30.00
-40.00
-50.00
-60.00
-70.00
0.00
40.00
80.00
120.00
160.00
200.00
240.00
FREQUENCY IN HZ ×10

FIG. 15

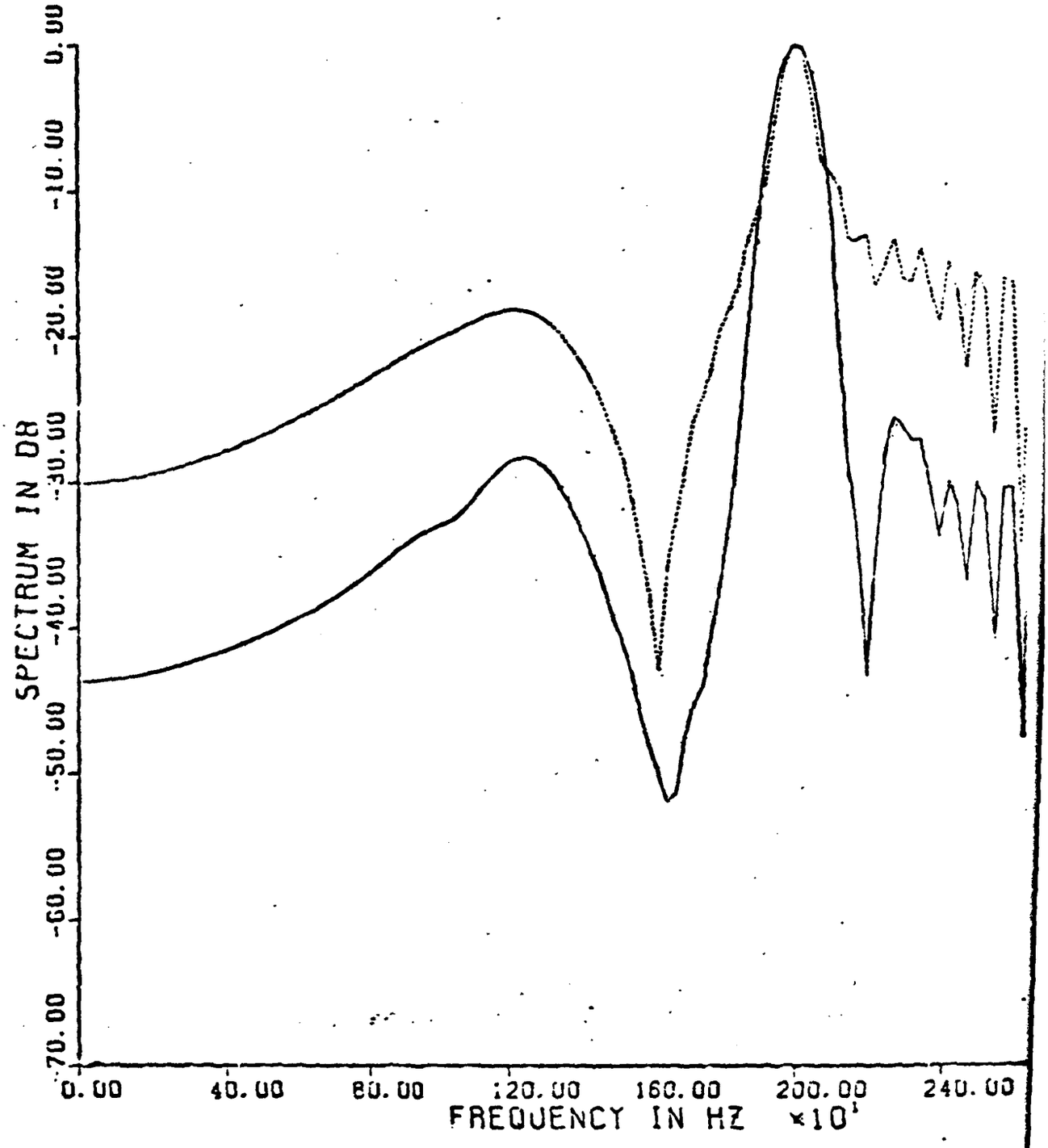
SPECTRUM IN DB
0.00
-10.00
-20.00
-30.00
-40.00
-50.00
-60.00
-70.00
0.00
40.00
80.00
120.00
160.00
200.00
240.00
FREQUENCY IN HZ ×10¹

FIG. 16

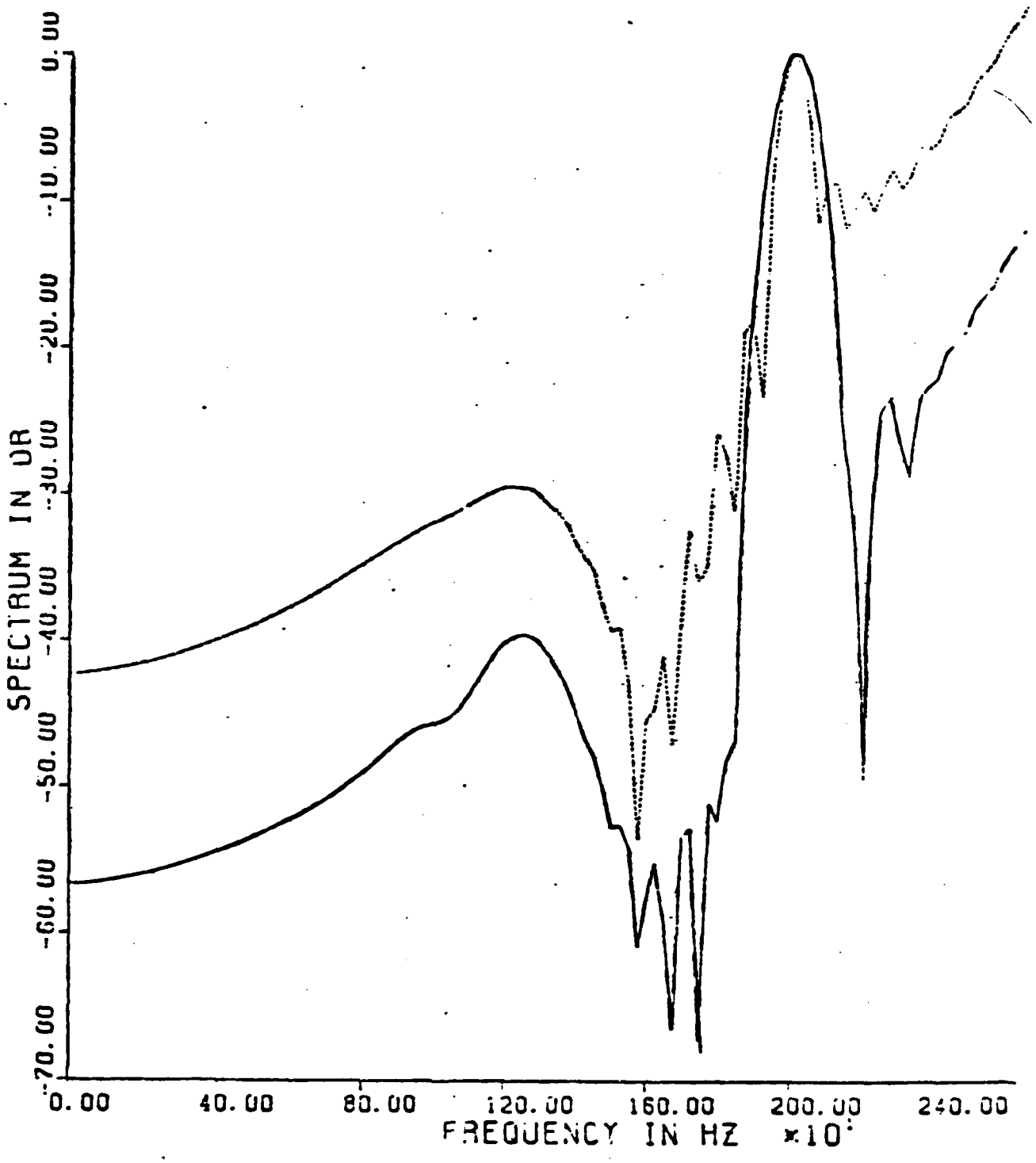
SPECTRUM IN DB
0.00
-10.00
-20.00
-30.00
-40.00
-50.00
-60.00
-70.00
0.00
40.00
80.00
120.00
160.00
200.00
240.00
FREQUENCY IN HZ ×10²

FIG. 17